VNU Journal of Science: Mathematics – Physics, Vol. 33, No. 1 (2017) 35-40

Crystal Structure and Magnetic Properties for $Bi_{1-x}Eu_xFeO_3$ Compounds

Ngo Thu Huong[1,2,*], Luu Hoang Anh Thu[1],
Nguyen Ngoc Long[1], Nguyen Hoa Hong[2]

[1]*Faculty of Physics, VNU University of Science, 334 Nguyen Trai, Thanh Xuan, Hanoi, Vietnam*

[2]*Nanomagnetism Laboratory, Department of Physics and Astronomy, Seoul National University, Seoul 151-747, South Korea*

Received 25 January 2017
Revised 18 February 2017; Accepted 20 March 2017

Abstract: $BiFeO_3$ (BFO) is a promising multiferroic material due to its high ferroelectric and antiferromagnetic ordering temperatures. Substituting partially Bi by Rare-Earth (RE) seem to be one way to enhance magnetization of BFO. In this study, crystal structure and magnetic properties for $Bi_{1-x}Eu_xFeO_3$ compounds are presented. When the Eu content was below 5% ($x < 0.05$), no significant improvement in magnetic properties was observed. However, when $x < 0.20$, ferromagnetism was induced. More particularly, at $x = 0.20$, the compounds experienced a drastically structural transition that governs also their optical properties.

Keywords: $BiFeO_3$; Rare-Earth-doping; Magnetic property; Raman.

1. Introduction

$BiFeO_3$ (BFO) is a promising multiferroic material because of its high ferroelectric (about 1100 K) and antiferromagnetic (about 650 K) ordering temperatures, much above room temperature. There are many reports on the magnetization enhancement of $BiFeO_3$ bulks, thin films, and nanoparticles, due to Bi-site substitution by selected trivalent rare-earth and divalent ions, or Fe-site substitution by transition metal ions. Liu *et al.* [1] suggested that the reason for higher magnetization after substitution of Eu^{3+} is the presence of the rare-earth orthoferrite impurity phase. Additionally, in certain cases, as reported by Qian *et al.* [2] for Dy^{3+} substitution, there is a large decrease in the particle size after substitution and this could be the reason for increased magnetization after substitution. Thakuria and Joy have shown that the ferromagnetic moment of the nanoparticles could be enhanced up to 3 times by the substitution of Bi by Ho. (However, the reported magnetization is still found only at quite high field, i.e. 6 T). From another aspect, it was found that the Curie temperature enhanced by 20 K if Bi was substituted by La [3].

* Corresponding author. Tel.: 84-943313567
Email: ngothuhuong2013@gmail.com

BFO has a rhombohedrally distorted perovskite-type crystal structure with lattice parameters of a_{hex} = 5.571 Å and c_{hex} = 13.868 Å at room temperature. The BFO unit cell can be described both hexagonal and pseudo-cubic. The pseudo-cubic representation of these rhombohedral cell parameters is a_{cubic} = 3.963 Å. The space group is determined as *R*3*c* with six formula units per hexagonal unit cell or two formula units per pseudo-cubic unit cell [4]. In this structure, the pseudo-cubic $[111]_c$ is equivalent to hexagonal $[001]_h$ [5]. According to A. Lahmar *et al.* [6], the reflections are indexed according to a pseudocubic, the lines (110) and (-110) observed in pure BFO are overlapped and shifted for all doped films. All other compositions are characterized by higher ferroelectric polarization but almost no magnetization. As reported by Zhenxiang Cheng *et al.*, the $Bi_{1-x}La_xFeO_3$ (x = 0, 0.1, 0.2 and 0.3) system were made by traditional solid state reaction. While for x = 0.1, the structure of BFO was maintained, for x = 0.2 the sample showed a change to C222 orthorhombic symmetry. With increasing La doping levels in BFO up to 30%, the system symmetry transformed to *P*4*mm* [7]. The magnetic moment of the samples was greatly improved with increasing La doping content in BFO. But all the samples crystallized in a rhombohedral distorted perovskite structure for $Bi_{0.9-x}La_{0.1}Pr_xFeO_3$ (x = 0, 0.1 and 0.2) ceramics. Some extra peaks of $Bi_2Fe_4O_9$ and $Bi_{46}Fe_2O_{72}$ were also observed. The H_c and M_r increase (1.7% and 3.5% respectively) with an increase in Pr doping [8]. According to S. Pattanayak *et al.* [7], for Sm-doped BFO systems, the lattice symmetry is rhombohedral (R3c) (for $x \leq 0.15$) to orthorhombic for x = 0.25. With increasing Sm-content of Sm-doped BFO, the position of peak shifts toward the higher angle region. The remnant magnetization increases with increase of Sm content. The magnetization in Sm-doped BFO should be related to an antisymmetric exchange mechanism [7]. For the Eu-doped BFO ceramics, Xingquan Zhang *et al.* showed that the structure had changed from rhombohedral to orthorhombic when Eu concentration was increased to 20% [9].

It seems that Eu doping could effectively improve the structural and magnetic properties of BFO compound. Thus, in this study, we investigate the influence of Eu^{3+} doping concentration on structural and magnetic properties of BFO ceramics.

2. Experiment

The $Bi_{1-x}Eu_xFeO_3$ ceramics (with x = 0; 0.01, 0.02, 0.03, 0.04, 0.05, 0.1, 0.15, and 0.2) were fabricated by a traditional solid state reaction. The starting materials were Bi_2O_3, Eu_2O_3 and Fe_3O_4, all with purity of 99,9%. The oxide materials were ground, pressed in to pellets and then sintered twice at 500^{o}C and 855 ^{o}C for 5 h, separately.

The structural analysis was performed by X-ray diffraction (XRD) with Cu K_α radiation. The surface morphology of the sintered pellets was examined by a Scanning Electron Microscope (SEM-JEOL- JSM5410LV). Raman scattering spectra were measured by Labram HR800 at room temperature. The magnetic measurements were performed by a Quantum Design Superconducting Quantum Interference Device (SQUID) system under magnetic field (H) from 0 up to 0.5 T under a range of temperatures (T) from 350 K down to 5 K.

3. Results and discussion

X-ray diffraction patterns of all the $Bi_{1-x}Eu_xFeO_3$ bulk samples are investigated. Figure 1 shows the XRD patterns for samples with x = 0.0; 0.05; 0.10; 0.15 and 0.20. It can be seen that all the samples are single phase, except for the sample with x = 0.05 (other impurity phase $Bi_2Fe_4O_9$ exhibited). When $x \leq 0.15$, samples characterize a polycrystalline rhombohedral structure with R3c space group. For the

sample with x = 0.20, it is obvious that the XRD pattern is orthorhombic lattice type with *Pnma* space group $EuFeO_3$ [10], suggesting a structural phase transition at x = 20%.

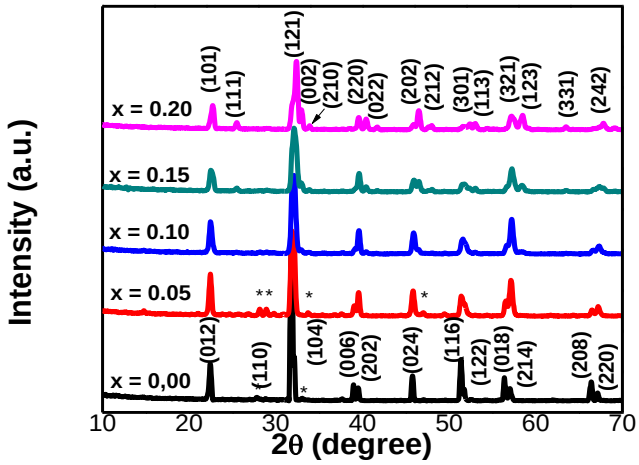

Fig. 1. X-ray diffraction patterns for the $Bi_{1-x}Eu_xFeO_3$ bulk samples (x = 5, 10, 15, 20%).

The typical parameters are shown in Table 1. The lattice constants decrease with increasing Eu concentration. The structural change of these compounds is also clearly in the Raman spectra that will be discussed later.

Table 1. Structural parameters for $Bi_{1-x}Eu_xFeO_3$ ceramics

x	Structure	Space group	A (Å)	b (Å)	c (Å)	Volume (Å^3)	D (nm)
x = 0.00	Rhombohedral	*R3c*	5.574	5.574	13.854	372.71	27
x = 0.05	Rhombohedral	*R3c*	5.569	5.569	13.828	371.44	15
x = 0.10	Rhombohedral	*R3c*	5.560	5.560	13.792	369.28	15
x = 0.15	Rhombohedral	*R3c*	5.553	5.553	13.761	367.522	14
x = 0.20	Orthorhombic	*Pnma*	5.622	7.799	5.441	238.51	16

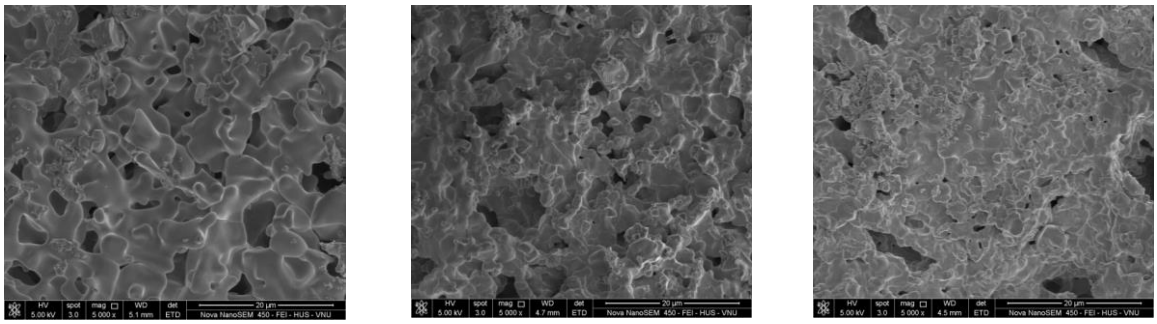

a) x = 0.0 b) x = 0.10 c) x = 0.20

Fig. 2. SEM images for $Bi_{1-x}Eu_xFeO_3$ bulk samples: a) x = 0; b) x = 0.10; c) x = 0.20.

SEM images for $Bi_{1-x}Eu_xFeO_3$ ceramic samples (with x = 0.0; 0.10 and 0.20) show in Fig. 2. When increasing the Eu concentration, the sample's surface seems to be smoother and the particle size is smaller.

Fig. 3 shows the Raman spectra for the undoped BFO and the $Bi_{1-x}Eu_xFeO_3$ ceramics. According to group theory, the undoped BFO should have the rhombohedral *R*3c structure with thirteen oscillation modes, which are $4A_1 + 9E$ [11-20].

In the Raman spectra of our BFO samples, one can observe three peaks as of A_1-1 (LO), A_1-2 (LO) and A_1-3 (LO) in the low frequency region, at 136.9 cm^{-1}; 172.1 cm^{-1} and 221.7 cm^{-1}, respectively and eight vertical E (TO) in the higher frequency region at 261.4 cm^{-1}; 274.4 cm^{-1}; 346.2 cm^{-1}; 369.2 cm^{-1}; 434.1 cm^{-1}; 474.9 cm^{-1}; 519.8 cm^{-1} and 620.6 cm^{-1} (Refer Fig. 3 and Table 2). From Fig. 3 one can see that with increasing the Eu concentrations (from 0.00 to 0.15), the oscillation mode intensity decreases and the peak shift, namely the vertical A_1- 1; A_1-2; A_1-3; 261.4; 274.4; 369.2 and 519.8 cm^{-1} shift towards to higher frequencies, while 620.6 cm^{-1} peak shifts towards to lower frequencies (Table 2). For x = 0.2, Raman spectrum completely changes in spectral appearance with new peaks at 223.2 cm^{-1}; 288.9 cm^{-1}; 400.6 cm^{-1}; 489.9 cm^{-1} and 601.6 cm^{-1}.The A_1-1, A_1-2 and A_1-3 oscillation modes in BFO are supposed to be related to inter-covalent Bi - O [15,17,18]. When the Eu^{3+} ions replace the Bi^{3+} ions, the percentage of covalent linkages Bi - O will decrease, leading to a decreasing in the peak intensity increases as the concentration of Eu changed. Additionally, the distortion network as well as defects in the crystal lattice of the doped samples can also cause some decrease in the peak intensity.

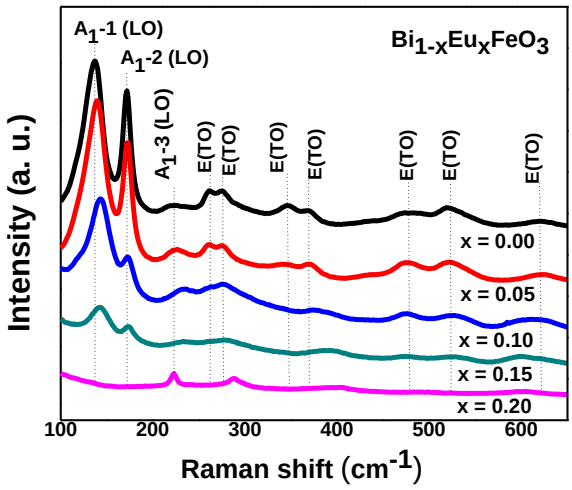

Fig. 3. The Raman spectra for the $Bi_{1-x}Eu_xFeO_3$ ceramics.

We know that the Raman scattering frequency is very sensitive to the movement of atoms, i.e. it strongly depends on local factors such as constant ionic strength and volume. If k is the force constant and M is the atomic mass, the oscillation frequency is proportional to $(k/M)^{1/2}$ [12, 20]. Since the radius of the Eu^{3+} ion (1.066 Å) is approximately equal to the radius of Bi^{3+} ion (1.17 Å), the force constant is not changed much when Eu^{3+} ion replaces the Bi^{3+} ion. However, the atomic mass of Eu (151.96 g/mol) is quite small that of the Bi (208.98 g/mol), thus, replacing Bi^{3+} ion by ion Eu^{3+}, which is lighter, will lead to an increase of the oscillation mode frequency as observed.

Table 2. Raman frequencies of the undoped BFO and $Bi_{1-x}Eu_xFeO_3$ compounds.

x	A_1-1 (cm^{-1})	A_1-2 (cm^{-1})	A_1-3 (cm^{-1})	E (cm^{-1})	E (cm^{-1})	E (cm^{-1})	E (cm^{-1})	E (cm^{-1})	E (cm^{-1})	E (cm^{-1})	E (cm^{-1})
0.00	136.9	172.1	221.7	261.4	274.4	346.2	369.2	434.1	474.9	519.8	620.6
0.05	139.1	172.1	225.5	260.7	274.4	344.0	369.2	435.0	475.4	522.0	622.1
0.10	143.0	172.8	233.9	262.2	275.2	-	375.3	-	475.4	525.1	613.0
0.15	142.2	173.5	234.7	-	277.5	-	389.8	-	474.7	525.8	599.2
0.20	-	-	223.2	-	288.9	-	400.6	-	489.9	-	601.6

Magnetization versus magnetic field taken at 300 K for all the samples is shown in Fig. 4a. It is seen that there is no significant improvement in magnetic properties when Eu^{3+} concentration is less than 5% at, i.e. the samples are paramagnetic at room temperature.

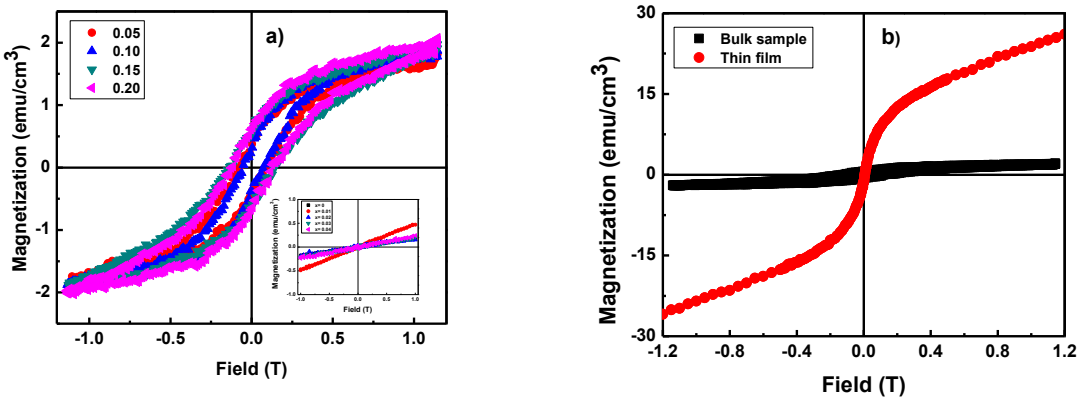

Fig. 4. Magnetization versus magnetic field taken at 300 K for (a) the $Bi_{1-x}Eu_xFeO_3$ samples (x = 0,05, 0,10, 0.15, 0.20), and (b) for the $Bi_{0.8}Eu_{0.2}FeO_3$ ceramic and thin film. The inset of Fig. 4(a) shows paramagnetic behavior of Eu-doped BFO with the Eu content below 0.05.

When the Eu concentration increases above 5%, all the samples show ferromagnetic behavior. Now, there has been almost no report of room temperature ferromagnetism in Rare-Earth-doped BFO ceramics. Even if the magnetic moment is one order smaller to that of films with the same concentrations (x = 0.20) (see Fig. 4b), the ferromagnetism in Eu-doped BFO ceramics is significant. Thin films should be a way to enhance the magnetic moment due to taking advantage of nano-structured magnetism and/or better texture/orientation that help magnetization along easy axis.

4. Conclusion

We have doped Eu^{3+} for Bi in BFO ceramics. It is shown that Eu doping can induce room temperature into BFO ceramics of the Eu content is greater than 5%. More particularly, at 20% of doping, the Eu-doped BFO compounds have gone through a drastically structural transition that governs strongly their optical behaviors. There is an important relationship between structural, magnetic, and optical properties in Eu-doped BFO ceramics. Our results may help to find an appropriate dopant concentration for different purposes of applications.

Acknowledgements

N. T. Huong would like to thank KFAS for her fellowship of academic year 2013-2014 and the BK 21 PrograSm of Department of Physics and Astronomy, SNU, for the fellowship of academic year 2014-2015.

References

[1] J. Liu, L. Fang, F. Zheng, S. Ju, and M. Shen, Appl. Phys. Lett. 95, 022511 (2009).
[2] F. Z. Quian, J. S. Jiang, S. Z. Guo, D. M. Jiang, and W. G. Zhang, J. Appl. Phys. 106, 084312 (2009)
[3] P. Thakuria and P. A. Joy, Appl. Phys. Lett. 97, 162504 (2010).
[4] I. Sosnowska , T. Peterlin-Neumaier and E. Steichele , J. Phys. C: Solid State Phys. 15, 4835 (1982).
[5] V. V. Lazenk, G. Zhang, J. Vanacken, I. I. Makoed, A. F. Ravinski and V. V. Moshchalkov J. Phys. D: Appl. Phys. 45, 125002 (2012).
[6] A. Lahmar, S. Habouti, M. Dietze, C.-H. Solterbeck, and M. Es-Souni, Applied Physics Letters 94, 012903 (2009).
[7] S. Pattanayak, R. N. P. Choudhary, and P. R. Das, Electron. Mater. Lett., Vol. 10, No. 1 pp. 165-172 (2014).
[8] P. Uniyal and K. L. Yadav, J. Phys.: Condens. Matter 21, 405901 (2009).
[9] X. Zhang, Y. Sui, X. Wang, Y. Wang, Z. Wang, J. Alloys and Compounds 507, 157–161 (2010).
[10] S.Z. Li, Y.J. Huang, J.B. Zhu, Y. Zhang, N. Chen, Y.F. Hsia, Phys. B: Condens. Matter. 393, 100 (2007).
[11] M. Cazayous, D. Malka, D. Lebeugle, and D. Colson, Appl.Phys. Lett. 91, 071910 (2007).
[12] G. L. Yuan, Siu Wing Or, and Helen Lai Wa Chan, J. Appl. Phys. 101, 064101 (2007).
[13] Y. Yang, J. Y. Sun, K. Zhu, Y. L. Liu, and L. Wan, J. Appl. Phys. 103, 093532 (2008).
[14] M. N. Iliev, M. V. Abrashev, D. Mazumdar, V. Shelke, and A. Gupta, Phys. Rev. B 82, 014107 (2010).
[15] Yang Yang, Liu Yu-Long, Zhu Ke, Zhang Li-Yan, Ma Shu-Yuan, Liu Jie, and Jiang Yi-Jian, Chin. Phys. B 19, 037802 (2010).
[16] T. Karthik, T. Durga Rao, A. Srinivas, and Saket Asthana, arXiv:1206.5606v1 (2012).
[17] T. Durga Rao, T. Karthik, Adiraj Srinivas, Saket Asthana, Solid State Comm. 152, 2071 (2012).
[18] Ya-nan Zheng, Yu-jie Wu, Zhen-xing Qin, Xiao-jia Chen, Chin. J. Chem. Phys., 26, 157 (2013).
[19] Anju Ahlawat1, S. Satapathy, V. G. Sathe, R. J. Choudhary, M. K. Singh, Ravi Kumar, T. K. Sharma, P.K.Gupta, arXiv:1306.4214v1 (2013).
[20] T. Durga Rao, T. Karthik, Saket Asthana, Journal of Rare Earths, 31, 370 (2013).